Facultative and anaerobic consortia of haloalkaliphilic ureolytic microorganisms capable of precipitating calcium carbonate

Dana J. Skorupa[1,2], Arda Akyel[1,2], Matthew W. Fields[2,3], and Robin Gerlach[1,2†]

[1]Department of Chemical and Biological Engineering, Montana State University, Bozeman, MT, 59717, USA

[2]Center for Biofilm Engineering, Montana State University, Bozeman, MT, 59717, USA

[3]Department of Microbiology and Immunology, Montana State University, Bozeman, MT, 59717, USA

Abbreviated Running Headline: Facultative and anaerobic MICP

† Corresponding author: Robin Gerlach, Montana State University, 59717-3980, PO Box 173920, Room 314 Cobleigh Hall, Bozeman, MT, USA.

E-mail: robin_g@montana.edu

Abstract

Aims: Development of biomineralization technologies has largely focused on microbially induced carbonate precipitation (MICP) via *Sporosarcina pasteurii* ureolysis; however, as an obligate aerobe, the general utility of this organism is limited. Here, facultative and anaerobic haloalkaliphiles capable of ureolysis were enriched, identified and then compared to *S. pasteurii* regarding biomineralization activities.

Methods and Results: Anaerobic and facultative enrichments for haloalkaliphilic and ureolytic microorganisms were established from sediment slurries collected at Soap Lake (WA). Optimal pH, temperature, and salinity were determined for highly ureolytic enrichments, with dominant populations identified via a combination of high-throughput SSU rRNA gene sequencing, clone libraries, and Sanger sequencing of isolates. The enrichment cultures consisted primarily of *Sporosarcina*- and *Clostridium*-like organisms. Ureolysis rates and direct cell counts in the enrichment cultures were comparable to the *S. pasteurii* (strain ATCC 11859) type strain.

Conclusions: Ureolysis rates from both facultatively and anaerobically enriched haloalkaliphiles were either not statistically significantly different to, or statistically significantly higher than, the *S. pasteurii* (strain ATCC 11859) rates. Work here concludes that extreme environments can harbor highly ureolytic active bacteria with potential advantages for large scale applications, such as environments devoid of oxygen.

Significance and Impact of the Study: The bacterial consortia and isolates obtained add to the possible suite of organisms available for MICP implementation, therefore potentially improving the economics and efficiency of commercial biomineralization.

Keywords biomineralization, bio-inventory, haloalkaliphile, ureolysis activity, calcium carbonate.

Introduction

Biomineralization is the generation of minerals by living organisms. Mineral precipitation can occur either directly or indirectly, with indirect synthesis arising when intracellular metabolic activities within a cell result in extracellular supersaturation and mineral precipitation. The best studied example of indirect mineral production likely is microbially induced calcium carbonate precipitation (MICP), where the microbially-driven hydrolysis of urea results in the production of ammonia (NH_3) and dissolved inorganic carbon (DIC) (eq 1). The reaction increases pH and carbonate alkalinity (eq 2 and 3) and favors the precipitation of $CaCO_3$ when dissolved calcium is present (eq 4; Lauchnor et al., 2013).

$$NH_2CONH_2 + 2H_2O \rightarrow 2NH_3 + CO_2 \quad (1)$$

$$2NH_3 + 2H_2O \leftrightarrow 2NH_4^+ + OH^- \quad (2)$$

$$CO_2 + 2OH^- \leftrightarrow HCO_3^- + OH^- + CO_3^{2-} + H_2O \quad (3)$$

$$Ca^{2+} + CO_3^{2-} \rightarrow CaCO_3\ (s) \quad (4)$$

The process is applicable to numerous engineered applications, from carbon sequestration (Mitchell et al., 2010) and groundwater remediation (Achal et al., 2012), to soil stabilization (Whiffin et al., 2007) and improved subsurface barriers (Rusu et al., 2011). The most common organism used in subsurface engineered biomineralization applications is the ureolytic bacterium *Sporosarcina pasteurii* (Phillips et al., 2013). By injecting this organism into the subsurface in combination with a supply of dissolved calcium and urea, the precipitation of calcium carbonate ($CaCO_3$) in the surrounding environment, allows for small leaks in porous rock formations to be sealed or porous media, such as soils, to be stabilized. *S. pasteurii* produces significant amounts

of urease (Ferris et al., 1996; Stocks-Fisher et al., 1999; DeJong et al., 2006) and is effective at mineralization across a variety of size scales (*e.g.*, summarized in Phillips et al., 2013; Phillips et al., 2016). However, the long-term use of tested laboratory strains under field-relevant conditions and their tolerance to the pressures, temperatures, salt concentrations, and oxygen conditions observed in the deeper subsurface is a challenge (Martin et al., 2012; Martin et al., 2013).

Recent work has shown *S. pasteurii* to be incapable of growth in the absence of oxygen (Martin et al., 2012), indicating that repeated injections of the organism would be required to maintain long term biomineralization in anoxic subsurface environments. As well, though *S. pasteurii* is capable of growth in sea water (Mortensen et al., 2011), deep aquifers can contain significantly higher salinity levels (Bassett and Bentley, 1983) potentially resulting in urease inhibition. Urease activity is also known to be pH-dependent, with a pH of approximately 7 being described as optimal for known enzymes (Fidaleo and Lavecchia, 2003). This pH dependence could inhibit the biological activity of organisms like *S. pasteurii* in the subsurface because water associated with well cement can routinely have pH values between 11 and 13 (Bang et al. 2001; Jonkers et al. 2010). These limitations with *S. pasteurii* create a need to isolate alternative microorganisms adapted to the extreme conditions potentially encountered in the deep subsurface.

This study examines the ability of haloalkaliphilic organisms to perform ureolysis-induced $CaCO_3$ precipitation under either (initially) low-oxygen ('facultative') or anaerobic conditions. The primary objectives were (1) to enrich urea-hydrolyzing microorganisms naturally adapted to high salinity, alkaline, and anoxic environments, thus selecting for ureolytic organisms adapted to conditions likely to be encountered in deep sub-surface rock formations; (2) identify the dominant microbial populations and morphologies using DNA sequencing and microscopy; and (3) compare

92 the ureolytic activity of haloalkaliphilic enrichment cultures to the current MICP model organism,
93 *S. pasteurii*.

94

95 **Materials and Methods**

96 *Site Description, aqueous chemical analyses, and biomass collection*

97 Sediment slurry samples were collected for microbial enrichments from three different locations
98 within or adjacent to Soap Lake, a meromictic, alkaline, saline lake located in central Washington,
99 USA. Sampling was conducted in January 2015 at locations identified as SL2 (47.24340 N,
100 119.29412 W), SL3 (47.31394 N, 119.29594 W), and SL4 (47.30770 N, 119.30006 W). Biomass
101 was collected by aseptically gathering a soil and/or sediment slurry and transferring it into a sterile
102 50 mL conical tube. Following collection, samples were maintained at 4°C until cultures could be
103 established. The temperature, pH, and electrical conductivity of each site was measured *in situ*
104 using a combined pH-temperature probe and meter-compatible electrical conductivity probe (YSI
105 Incorporated, Yellow Springs, OH).

106 Aqueous geochemistry was also assessed at sites SL2 and SL3; the sample from site SL4
107 consisted of solid material only (top soil from a salt flat) and therefore no aqueous geochemistry
108 data are available. Briefly, site water was filter-sterilized (0.22 μm) directly into sterile 50 mL
109 conical tubes. Some filtered site water was acidified in the field with 5% trace metal grade nitric
110 acid prior to transport and used for total dissolved metals analysis. Concentrations of total metals
111 were measured using an Agilent 7500ce ICP-MS by comparing to certified standards (Agilent
112 Technologies, Environmental Calibration Standard 5183-4688). Ion chromatography was used to
113 determine concentrations of dominant anions. For this, non-acidified filtered samples were
114 analyzed using a Dionex ICS-1100 chromatography System (Dionex Corp., Sunnyvale, CA)

equipped with a 25 µL injection loop and an AS22-4x250 mm anion exchange column, using an eluent concentration of 4.5 mmol l^{-1} sodium carbonate and 1.4 mmol l^{-1} sodium bicarbonate flowing at a rate of 1.2 mL·min^{-1}. An overview of the aqueous geochemistry is given in Table S1; the following were not detected NO_2^-, Br^-, PO_4^{3-}, and dissolved Fe.

Samples were also collected for total community analysis by filtering 2 L of site water from each sampling location through a 0.22 µm filter. The filters were aseptically transferred into a 50 mL conical vial, immediately placed on dry ice, and stored at -80ºC until DNA extraction.

Enrichment, Optimal Growth Conditions, and Microbially-Induced $CaCO_3$ Precipitation Activity

Calcium mineralizing medium (CMM) was used to enrich ureolytic bacteria. The medium consisted of 3 g l^{-1} Difco Nutrient Broth (BD, Sparks MD), 333 mmol l^{-1} urea, 187 mmol l^{-1} NH_4Cl, and was modified with both 0.077 mmol l^{-1} $NiCl_2$ and 50 g l^{-1} NaCl. The medium was prepared either anaerobically (N_2 headspace) or aerobically, pH adjusted to 9 with 5 mol l^{-1} NaOH, distributed into 30 mL Hungate tubes sealed with butyl-rubber stoppers, and sterilized by autoclaving. Enrichment cultures were established in triplicate by inoculating Hungate tubes containing 9 mL of autoclaved CMM medium with 1 mL of environmental sediment slurry (10% [vol·vol^{-1}]) and incubation at 37ºC without shaking. Enrichments were screened for ureolytic activity by monitoring urea concentrations in filtered (0.22 µm filter) subsamples using a modified Jung assay (Jung et al., 1975; Phillips et al., 2016). Enrichment cultures positive for ureolysis were transferred into fresh medium for continued cultivation.

Subsequent experiments investigating $CaCO_3$ precipitation efficacy used CMM medium with the pH adjusted to 6 prior to autoclaving. The medium was amended with 33 mmol l^{-1} sterilized $CaCl_2 \cdot 2H_2O$ prior to inoculation with 10% [vol·vol^{-1}] of culture before static incubation at 30ºC. Liquid samples were collected every two hours, passed through a 0.22 µm filter and

analyzed for pH and dissolved concentrations of urea using a modified Jung assay (Jung et al., 1975; Philips, 2013a). Dissolved levels of Ca^{2+} were measured using filtered samples and were determined via spectrophotometry measurements at 620 nm using a modified calcium-*o*-cresolphthalein complexome method (Kanagasabapathy and Kumari, 2000). Alkalinity was tracked after diluting samples (1:50) in water (18.2 MΩ.cm) and titrating with HCl (0.1 mol l^{-1}) to a pH of 4.5 using an automatic titrator (HI 902, Hanna Instruments, Woonsocket, RI). Mineral precipitates were dried and characterized at the end of the experiment using a LabRAM HR Evolution Confocal Raman microscope (Horiba Scientific, France) at 100-500x magnification and a 532 nm laser (100 mW). Spectra were collected over a 100-2000 cm^{-1} range using an 1800 gr/mm grating and a 1024 x 256 pixel air cooled CCD detector. Peak identification was supported using the KnowItAll Raman spectra library (Bio-Rad, Hercules, CA).

CMM medium was also utilized to determine the optimal temperature, pH and salt concentrations for established ureolytic enrichments. Cultures were incubated at 20, 25, 30, 37, 40, and 45ºC without shaking to determine the optimal growth temperature. After determining the optimal growth temperature, the effects of pH on growth were monitored by poising the pH at values ranging from 6.0 to 11.0 using either NaOH or HCl. Finally, optimal salt concentrations were determined by varying NaCl levels between no addition and 4.3 mol l^{-1} using the optimal growth temperature and pH value. Treatments were monitored for growth by collecting optical density measurements at 600 nm (Unico, S-1100 VIS spectrophotometer, 1 cm path length). Identical physiological tests were also conducted on a pure culture of the model MICP strain *S. pasteurii* (ATCC 11859) during growth in Brain Heart Infusion (BHI) medium (Becton Dickinson).

Urea hydrolysis kinetics of haloalkaliphilic enrichment cultures were compared to those of the model MICP strain *S. pasteurii* (strain ATCC 11859) using CMM containing 333 mmol l^{-1} urea. CMM was inoculated with a 10% [vol·vol^{-1}] culture volume, and urea concentrations were tracked using the modified Jung assay described above. Changes in total cell numbers were monitored using acridine orange staining and direct cell counting. Briefly, 1.98 mL of sample was mixed with 20 µl acridine orange (40 mg·mL^{-1}) and incubated at room temperature for 30 minutes before rinsing with nanopure water. The stained sample was filtered onto a black polycarbonate 0.22 µm membrane filter, washed with nanopure water, dried and mounted on a microscope slide using immersion oil. Slides were viewed using a transmitted/epifluorescence light microscope (Nikon Eclipse E800) with an Infinity 2 color camera with the appropriate filter set. A total of 10-30 microscopy fields were counted for each sample slide.

DNA extraction, PCR, and sequencing

DNA for total community analysis was extracted from each collected Soap Lake filter using a modified version of the FastDNA Spin Kit for Soil (MP Biomedicals, Solon, OH). Frozen filters were aseptically cut in half, with one half placed in a sterile petri dish for DNA extraction. Unused sections of the filter were stored at -80ºC. The half filter was further cut into smaller pieces and aseptically transferred to a Lysing Matrix E tube. DNA was also extracted from facultative and anaerobic ureolytic enrichments to identify cultivated species. Briefly, 30 mL of enrichment culture was harvested by centrifugation, the pellet re-suspended in the provided MP Biomedicals phosphate buffer and transferred to a Lysing Matrix E tube. The DNA extraction for both the filters and enrichment sample types then continued according to the manufacturer's instructions. Following extraction, the DNA from the filter and enrichment samples was cleaned and concentrated using a OneStep™ PCR Inhibitor Removal Kit (Zymo Research, Irvine, CA) and

183 Qiaquick PCR Purification Kit (Qiagen, Valencia, CA). DNA extraction from axenic isolates
184 followed the protocol outlined by Lueders et al. (2004), and following extraction all samples were
185 purified using the Qiaquick kit referenced above.
186 The V1V2 and V3 regions of the bacterial SSU rRNA gene were targeted for total
187 community analysis using the universal bacterial primers 8F (5'-
188 AGAGTTTGATCCTGGCTCAG- 3′) and 529R (5'- CGCGGCTGCTGGCAC- 3'). The forward
189 and reverse primers contained an Illumina Nextera XT overhang sequence that allowed for
190 addition of multiplexing indices in a downstream PCR. Each 20 µL PCR mixture contained
191 approximately 1-5 ng of DNA, 0.001 mmol l^{-1} of each primer, 2 µg of BSA, and 10 µL of KAPA
192 HIFI HotStart ReadyMix (Kapa Biosystems Inc., Wilmington, MA). The PCR program was
193 performed with the following cycling conditions: an initial denaturation at 95ºC (3 min), followed
194 by 25 cycles of denaturation at 98ºC (20 s), annealing at 58ºC (15 s), extension at 72ºC (30 s),
195 followed by a final extension at 72ºC for 5 minutes. Following verification of the amplicon product
196 in a 1.0% agarose gel, PCR products were cleaned and concentrated using the Qiaquick PCR
197 Purification Kit, and quantified using a Qbit fluorometer (Invitrogen, Carlsbad, CA). The
198 overhang-ligated amplicon products were further purified to remove free primers and primer
199 dimers using the AMPure XP bead kit (Beckman Coulter Inc., CA, USA) following the Illumina
200 instructions. Amplicons were subsequently barcoded using the Illumina Nextera XT index kit
201 (Illumina, San Diego, CA) and purified a second time using the AMPure XP bead kit. Purified
202 amplicon libraries were quantified using PicoGreen dsDNA reagent in 10 mmol l^{-1} Tris buffer (pH
203 8.0) (Thermo Fisher Scientific, Waltham, MA), pooled in equimolar amounts, spiked with 5%
204 PhiX control spike-in, and sequenced via the paired end platform (2 x 300 bp) on an Illumina

MiSeq® with the v3 reagent kit. Amplicon sequences are available in the following GenBank SRA accession SRP127176.

Near full-length amplification of the SSU rRNA gene sequences was performed for DNA obtained from enrichment cultures and axenic isolates using primers 8F (see above) and 1492R (5'-TACGGYTACCTTGTTACGACTT- 3') and the following PCR program: initial denaturation at 94ºC (2 min), followed by 25 cycles of denaturation at 94ºC (15 s), annealing at 51ºC (15 s), extension at 72ºC (100 s), and a final extension at 72ºC for 5 minutes. Amplicons were cloned using the CloneJet PCR Cloning Kit (ThermoFisher Scientific, Waltham, MA) and 25 clones were sequenced at the Molecular Research Core Facility at Idaho State University in Pocatello, ID, USA. The near full-length clone sequences are deposited as GenBank accessions MG682464-MG382488. Along with enrichment sequencing, pure cultures were obtained from each enrichment through sequential streaking (≥ 3 times) for isolation on solid BHI plates with 333 mmol l^{-1} urea and incubation at 30ºC. Following isolations, one pure culture derived from the facultative and one from the anaerobic enrichment was targeted for full-length SSU rRNA gene sequencing using the primers and thermocycler conditions described above. The near full-length clone sequences can be found as GenBank accessions MG674285-MG674286.

Pyrosequencing data and statistical analysis

The SSU rRNA gene amplicon sequences for total community analysis were quality trimmed and refined using the Mothur pipeline following the Schloss laboratory's standard operating procedure (SOP) for MiSeq data sets (Kozich et al., 2013). In brief, the programs make.contigs and screen.seqs (maximum number of ambiguous bases = 0, maximum length = 550 bp), were used to identify high quality sequences. Duplicate sequences were removed to reduce computational times, and unique sequences were aligned to a reference alignment using the SILVA 16S rRNA gene

sequences from *Bacteria*. This alignment was customized to the area immediately surrounding the V1V2 and V3 regions. Poorly aligned as well as chimeric sequences were identified and removed from the data set. Next, taxonomic classifications were assigned using classify.seqs, and sequences identified as derived from either the domain *Archaea* or the chloroplast/mitochondria organelle were removed. To further reduce computation times, groups with sequences present at less than 0.1% abundance were removed, thus focusing the analyses on abundant community members. These sequences were then binned into OTUs using the programs dist.seqs and cluster, and a representative sequence from each OTU was selected.

Representative sequences, near full-length clone libraries, and SSU rRNA gene sequences from isolated organisms were identified by comparison with known sequences in GenBank using BLASTn (http://blast.ncbi.nlm.nih.gov/Blast.cgi). Representative pyrosequencing reads were genus-level matches if they were ≥ 80% identical over ≥ 80% of the length of the read, while full-length clones were species-level matches if they were ≥ 97% identical over ≥ 80% of the length of the sequence.

Scanning Electron Microscopy

Facultative and anaerobic enrichments were grown in CMM medium without NaCl for microscopy. The cells were prepared for imaging by immobilization on a glass slide and then mounted and coated with iridium for imaging (1 kV) with a Zeiss Supra 55 Field Emission Scanning Electron Microscope (FE-SEM) at the Image and Chemical Analysis Laboratory (ICAL) at Montana State University.

Results

Habitat and Enrichment

Enrichment cultures for ureolytic microorganisms were prepared using sediment slurry samples collected at three shore-line locations at Soap Lake (site SL2), Alkali Lake (Site SL3), and Lenore Lake (Site SL4), a series of saline and alkaline lakes located in central Washington (Figure S1A). The pH values ranged between 9.05 and 9.85, with all water temperatures at 2ºC. CMM containing urea was inoculated in triplicate with sediment slurries and incubated in the dark at 37ºC without shaking. Abiotic controls without inoculum were also tracked alongside the enrichment cultures. Significant ureolysis (defined as ≥50% decrease in the urea concentration) was detected after 30 days in the facultative and anaerobic enrichments established from site SL2 sediment slurries (Figure S1B), and positive cultures were transferred into fresh medium. Abiotic controls showed no decrease in urea concentrations after 30 days. In an initial set of experiments, ureolysis efficacy and mineral precipitation were assessed in both the anaerobic and facultative SL2 enrichments by tracking urea, Ca^{2+}, and alkalinity levels over a ten-hour period. Decreases in urea (Figure 1A) and an increase in both medium pH (Figure 1B) and alkalinity (Figure 1D) indicated that ureolysis occurred in both enrichment cultures and that carbonate was produced. A roughly 33% reduction in the starting concentration of urea (333 mmol l^{-1}) was observed over 10 hours. This, combined with the observation of increased pH and alkalinity, verified that significant ureolysis occurred, resulting in the alkaline microenvironment necessary for carbonate mineral precipitation. Dissolved Ca concentrations were also tracked and used as a proxy for $CaCO_3$ precipitation (Figure 1C). Initial Ca concentrations were approximately 0.033 mol l^{-1} $CaCl_2 \cdot 2H_2O$. Ca concentrations decreased below the detection limit by the end of the 10-hour experiment (Figure 1C) in both enrichments, indicating that less than $1.25 \cdot 10^{-4}$ mol l^{-1} of the initial Ca concentration remained. Finally, mineral precipitates were characterized using Raman Spectromicroscopy, which identified calcite ($CaCO_3$) as main mineral phase in all samples

(Figure S2). The abiotic control samples showed no visible precipitates, and thus were not analyzed using Raman Spectromicroscopy.

Optimal Growth Conditions and S. pasteurii Tolerance Comparison

Facultative enrichments from site SL2 grew optimally at 30ºC but were capable of growth between 20ºC and 40ºC (Figure 2A). Similarly, the pH tolerance for this enrichment culture appeared to be broad, displaying growth across the entire pH 6-11 range at 30ºC (Figure 2A). The SL2 facultative enrichment also grew across a wide range of salinities (0-100 g l^{-1} NaCl) at 30ºC and a pH of 9, with optimal growth observed at 50 g l^{-1} (Figure 2D).

In contrast to the wide growth spectrum of the facultative enrichment, SL2 ureolytic enrichments cultivated under anaerobic conditions displayed a more restricted growth range. Limited growth was observed for the anaerobic SL2 enrichment after 24 hours across the entire tested temperature range (Figure 2B), though a slight preference for 30ºC was noted. The optimal and pH and salinity ranges were pH 8 at 30ºC and 25 g l^{-1} NaCl at 30ºC and pH 8, respectively (Figure 2B and 2E).

Additional experiments examined optimal conditions for *S. pasteurii* strain ATCC 11859 to determine its requirements and tolerance for growth under aerobic conditions. An initial set of experiments revealed that strain ATCC 11859 was incapable of growth in CMM medium that did not contain urea. Knowing that the inclusion of urea would initiate ureolysis, and significantly alter the pH of the medium, an alternative cultivation medium, BHI broth, was employed instead. Figure 2C shows that strain 11859 grew best at 30ºC, with a growth range of 22 to 40ºC. *S. pasteurii* strain 11859 also appeared to be adapted to alkaline environments, displaying significant growth at pH values ranging from 6 to 11 at 30ºC (Figure 2C). Finally, though optimum growth was achieved in the absence of additional NaCl, *S. pasteurii* strain 11859

297 appeared to be halotolerant, with growth observed in cultures with NaCl concentrations up to 75
298 g l^{-1} at 30°C and pH 8 (Figure 2F).

299 *Community Analysis*

300 Initial bacterial community characterizations were performed for site SL2 (Figure 3) and at
301 sampling locations SL3 and SL4 (Supporting Information Figure S3). Operational taxonomic
302 unit (OTU) richness (at 97% sequence identity) indicated a large proportion (67%) of the
303 baseline SL2 community were unclassified genera with predominant identified populations most
304 closely related to the well-known alkaliphilic bacterium *Microcella* (9% abundance), the
305 bacterium *Pullulanibacillus* (6% abundance), and the cyanobacterium *Synechococcus* (6%
306 abundance) (Figure 3). Shifts in genus-level relative abundance were apparent in the Illumina
307 SSU rRNA-based analysis following ureolytic enrichments, where *Bacillus* was the only genus
308 with an abundance of ≥1% in the facultative enrichment, while the obligate anaerobic
309 community was comprised of a mixture of *Bacillus* (39% abundance) and the obligate anaerobic
310 genus *Clostridium* (60% abundance) (Figure 3). This is in contrast to the baseline SL2
311 populations, where the genus *Bacillus* was present at approximately 3% abundance and
312 C*lostridium* populations were below 1% relative abundance.

313 Recent work taxonomically reclassified several *Bacillus* genera as belonging to the genus
314 S*porosarcina* based on distinct phylogenetic and cellular properties (Yoon et al., 2001). To
315 determine whether short Illumina sequence reads identified as *Bacillus* across the V1-V3 rRNA
316 gene region were potentially S*porosarcina* members, full-length SSU rRNA gene clones were
317 used to obtain species-level identification of enriched populations. All full-length clones from
318 the facultative ureolytic enrichment were a close gene sequence match (99% sequence similarity)
319 to *S. pasteurii* strain NCCB 48021 (Figure 3), while anaerobic SL2 enrichment clones were a

mixture of cultivated relatives of *Clostridium* sp. MT1 and *S. pasteurii* strain NCCB 48021 (Figure 3). For both enrichment cultures, the clone sequencing indicated that other potential organisms were present at abundance levels likely no greater than 4%. Along with these clone libraries, one isolate from each enrichment was analyzed via full-length rRNA gene sequencing. Results supported the clone library results, where both the facultative and anaerobic ureolytic isolates were a close gene sequence match (99% sequence similarity) to *S. pasteurii* strain NCCB 48021. SEM images of the enrichment cultures also support the genus-level identification, where numerous rod-shaped morphologies were detected under both culture conditions (Figure 4), which correlates to known morphologies for both *S. pasteurii* and *Clostridium*.

Rates of Precipitation

Urea concentrations and direct cell counts were tracked in SL2 enrichment cultures and the MICP type strain *S. pasteurii* ATCC 11859 to determine ureolytic activity on a per cell basis. Ureolytic activities were calculated by normalizing the moles of urea hydrolyzed per hour by the cell density. Interestingly, no lag phase in growth was detected in either of the SL2 enrichments, while growth of the MICP model strain *S. pasteurii* ATCC 11859 appeared to be delayed for approximately 2 hours following inoculation (Table 1). The obligate anaerobic enrichment communities from site SL2 displayed the highest cell-specific urea hydrolysis rates, peaking at $3.05 \cdot 10^{-10} \pm 2.40 \cdot 10^{-11}$ moles of urea hydrolyzed·cell^{-1}·hr^{-1} (Table 1). A two-tail Student's *t*-test assuming equal variances determined this activity level was statistically significant ($P < 0.01$) when compared to both the facultative SL2 enrichment as well as *S. pasteurii* ATCC 11859. Urea hydrolysis rates for the model MICP organism and the facultative SL2 enrichment cultures were comparable and averaged between $1.05 \cdot 10^{-10}$ to $1.95 \cdot 10^{-10}$ moles of urea hydrolyzed·cell^{-1}·hr^{-1}.

Discussion

One challenge identified in scaling up MICP-based sealing applications to the field lies in the availability of organisms adapted to the geochemical and geological conditions present in the deeper subsurface (Phillips et al. 2013, 2016). To date, biomineralization sealing studies have largely focused on the use of *S. pasteurii* strains, though its long-term persistence under anaerobic conditions is doubtful (Martin et al., 2012), and its ability to conduct ureolysis in deep saline aquifers is unknown (Mortensen et al., 2011). The work presented here enriched and identified bacterial populations, which increase the versatility and potential applicability of the biomineralization sealing technology beyond the current range. Using haloalkaliphilic media, either devoid of or containing minimal oxygen, we enriched for and identified ureolytically active bacterial populations potentially more suitable for deep subsurface environments.

An emerging need in commercializing biomineralization-based technologies is that suitable organisms be able to reliably precipitate $CaCO_3$ in anaerobic subsurface habitats. This study shows that enrichment of efficient facultative and anaerobic ureolytic bacteria from an alkaline soda lake environment may provide good alternatives to the obligate aerobic bacterium *S. pasteurii* ATCC 11859 or other reference strains. To date, anaerobic growth has only been observed using alternative carbonate mineral-forming metabolisms such as denitrification (van Paassen et al., 2010; Martin et al., 2012; Hamdam et. al., 2016), sulfate reduction (Wright and Wacey, 2005), and iron reduction (Zeng and Tice, 2014). Each one of these alternate metabolisms generally results in slower growth rates than aerobic respiration, and since mineral precipitation-inducing reactions for these metabolisms are growth-dependent, precipitation rates are generally slower. Urea hydrolysis can be growth-independent, thus the ability of an organism to promote high rates of ureolysis while growing in the absence of oxygen might be central to

reliably implementing ureolysis-induced mineral precipitation strategies in the deep subsurface. Along with the ability to promote growth and ureolysis anaerobically, work here also shows that it can occur across NaCl concentrations ranging from 0-100 g l^{-1}, and at pH values as high as 11 (Figure 2A, 2B, 2D, 2E). This indicates that the anoxic, high-pH, and high salinity conditions potentially present in deep saline aquifers could be suitable for the growth of ureolytic haloalkaliphilic organisms. Interestingly, by examining optimal growth conditions of the MICP model strain we also better defined the potential application range of *S. pasteurii* ATCC 11859 (Figure 2C, 2F), observing that it can reliably grow across salinities up to 75 g l^{-1}. This range far exceeds previously tested values which mimicked oceanic seawater (26.7 g l^{-1}) conditions (Mortensen et al., 2011) and supports the potential applicability of *S. pasteurii* to be used in deep (aerobic) saline aquifers which are a target environment for carbon capture and storage, as well as enhanced oil recovery.

Enrichment of haloalkaliphilic bacteria capable of hydrolyzing urea was not unexpected given the widespread detection of the *ure*C functional subunit in sediment and groundwater environments (Fujita et al., 2008), as well as the estimate that between 17 and 30% of cultivated species from soil habitats are capable of urea hydrolysis (Lloyd and Sheaffe, 1973). Previous work isolating ureolytic bacteria from soil habitats also observed that >50% of cultivated isolates were members of the *Sporosarcina* genus (Burbank et al., 2012), explaining the likelihood of enriching *S. pasteurii*-like strains. The inclusion of 333 mmol l^{-1} urea in the enrichment medium was also likely to result in conditions inhibitory to many species, due to the accumulation of ammonia and high pH values, thus potentially selecting for bacteria capable of constitutive urease expression and tolerance to high pH values and ammonium concentrations, of which few have been identified (Burbank et al., 2012).

Previous work demonstrated that *S. pasteurii* cannot synthesize urease under anaerobic conditions (Martin et al., 2012). In studies reported here, we enrich for a strain of *S. pasteurii* most closely related to strain NCCB 48021 under both facultative and obligate anaerobic conditions, therefore potentially overcoming known challenges with the deep subsurface application of the MICP model strain *S. pasteurii* ATCC 11859.

Along with *S. pasteurii*, a *Clostridium* species was also enriched in the anaerobic SL2 culture. Isolation of individual bacterial organisms was not a priority in the current work, as we envision utilizing mixed communities of biomineralizing microorganisms suited to specific down-hole environments for engineered applications. Using high-throughput SSU rRNA gene amplicon sequencing and clone libraries, obligate anaerobic ureolytic enrichment communities from site SL2 were observed to contain a mixture of a *S. pasteurii* strain most closely related to strain NCCB 48021 and a *Clostridium* sp. most closely related to strain MT1 (Figure 3). The enrichment of an obligate anaerobe like this *Clostridium* strain indicates that conditions in the enrichment culture were indeed anaerobic. While it is unclear whether enriched *Clostridium* populations were actively contributing to urea hydrolysis, several *Clostridium* species are known to be urease positive (Mobley and Hausinger, 1989), carrying their urease structural genes on a plasmid, and only activating urease gene expression under nitrogen deplete conditions (Dupuy et al., 1997). Further testing is needed to determine the potential functional role of *Clostridium* spp. in the anaerobic enrichment cultures.

The economic feasibility of MICP-based fracture sealing depends on high ureolytic activity and efficient $CaCO_3$ precipitation. To develop a bioinventory for field deployment, microorganisms must be able to remain ureolytically active, and ideally grow, under *in situ* conditions. These properties will help ensure subsurface leakage pathways are sealed in a

413 reasonable time frame. Results presented here indicate that the rate of urea removal on a per-cell
414 basis in the SL2 haloalkaliphilic anaerobic communities was statistically greater ($P < 0.01$) than
415 the *S. pasteurii* ATCC 11859 strain (Table 1), suggesting increased urea hydrolysis rates in the
416 anaerobic SL2 enrichment may well be due to higher urease enzyme activity on a per cell basis.
417 Interestingly, for both SL2 enrichment cultures, ureolysis started within the first two hours
418 following inoculation, and once initiated, took roughly 8 hours for >95% of 333 mmol l^{-1} urea to
419 be hydrolyzed (data not shown). Experiments here did not attempt to optimize either urea or Ca^{2+}
420 concentrations, both of which are parameters known to influence the $CaCO_3$ precipitation levels
421 (Krajewska 2018), suggesting further optimization of the MICP process is possible.
422 In summary, several challenges exist in continuing to move toward broader field-scale
423 implementations of MICP-based technologies. These challenges include costs associated with
424 the injection and growth of MICP organisms on a large scale, variability of conditions commonly
425 experienced in the subsurface, as well as ensuring proper biosafety and environmental
426 protections (Krajewska 2018; Ivanov et al., 2019). Knowing that saline aquifers are a primary
427 target for CO_2 sequestration and that subsurface fractures may serve as CO_2 leakage routes,
428 microorganisms used in MICP treatment need to be tailored to high-salinity and high-
429 temperature environments that are likely either microaerobic or completely anoxic. These saline
430 aquifers are also known to vary widely with respect to pH conditions. MICP has been used at
431 least twice to seal fractures at relevant depths (310-340 m) using the model organism *S. pasteurii*
432 (Phillips et al., 2016, 2018) in an environment that was moderately acidic (pH 5.5), brackish (24
433 g l^{-1} NaCl), and likely microaerophilic (-16 mV ORP). We present evidence here that highly
434 ureolytically active microbial communities with specific adaptation to high-pH and high-salinity
435 environments can be successfully isolated under anaerobic conditions, and that this consortium

of bacteria can add to the possible suite of organisms available for MICP implementation. We also show that extreme environments like those at Soap Lake can harbor microbial community members which produce large quantities of active urease, making them potentially useful for engineered biomineralization technologies. Further research and development efforts are needed to develop a collection of ureolytically active organisms suitable for the range of other conditions likely encountered at subsurface application sites, most notably increased temperature and pressure.

Acknowledgements

This research was supported by the U.S. Department of Energy (DOE) Small Business Technology Transfer (STTR) Program contract no. DE-FG02-13ER86571 ("Using Biomineralization Sealing for Leakage Mitigation in Shale during CO_2 Sequestration"). Arda Akyel was supported by the Thermal Biology Institute through funding from the MSU Office of the Vice President for Research and Economic Development for Ph.D. graduate enhancement. Our thanks are extended to Sara Altenburg for her help with SEM imaging, Dr. Erika J. Espinosa-Ortiz for confocal Raman Spectromicroscopy analysis, and Dr. Logan Schultz for sample collection.

Conflicts of Interest

The authors have no conflicts of interest to declare.

References

Achal V., Pan X., Fu Q., and Zhang D. (2012) Biomineralization based remediation of As(III) contaminated soil by *Sporosarcina ginsengisoli*. *J Hazard Mater* **201**, 178–184.

Bang S., Galinat J., and Ramakrishnan V. (2001) Calcite precipitation induced by polyurethane-immobilized *Bacillus pasteurii*. *Enzyme Microb Technol* **28**, 404–409.

Bassett R.L. and Bentley M.E. (1983) Deep brine aquifers in the palo duro basin: regional flow and geochemical constraints. *Bureau of Economic Geology* **130**, 1-59.

Burbank M.B., Weaver T.J., Williams B.C., and Crawford R.L. (2012) Urease activity of ureolytic bacteria isolated from six soils in which calcite was precipitated by indigenous bacteria. *Geomicrobiol J* **29**, 389-395.

DeJong J.T., Fritzges M.B., and Nüsslein K. (2006) Microbially induced cementation to control sand response to undrained shear. *J Geotech Geoenviron Eng* **132**, 1381–1392.

Dupuy B., Daube G., Popoff M.R., and Cole S.T. (1997) *Clostridium perfringens* urease genes are plasmid borne. *Infect Immum* **65(6)**, 2313-2320.

Ferris F., Stehmeier L., Kantzas A., and Mourits F. (1996) Bacteriogenic mineral plugging. *J Can Petrol Technol* **35**, 56–61.

Fidaleo M. and Lavecchia R. (2003) Kinetic study of enzymatic urea hydrolysis in the pH range 4–9. *Chem Biochem Eng Q* **17**, 311–318.

Fujita Y., Taylor J., Wendt L., Reed D., and Smith R. (2010) Evaluating the potential of native ureolytic microbes to remediate a (90)Sr contaminated environment. *Environ Sci Technol* **44**, 7652–7658.

Hamdam N., Kavazanjian Jr. E., Rittmann B.E., and Karatas I. (2016) Carbonate mineral precipitation for soil improvement through microbial denitrification. *Geomicrobiol J* 1-8.

Ivanov, V., Stabnikov, V., Stabnikova, O., and Kawasaki, S. (2019) Environmental safety and biosafety in construction biotechnology. *World J Microb Biot* **35**:26.

Jonkers H.M., Thijssen A., Muyzer G., Copuroglu O., and Schlangen E. (2010) Application of bacteria as self-healing agent for the development of sustainable concrete. *Ecol Eng* **36**, 230–235.

Jung D., Biggs H., Erikson J., and Ledyard P.U. (1975) New colorimetric reaction for end-point, continuous-flow, and kinetic measurement of urea. *Clin Chem* **21(8)**, 1136-1140.

Kanagasabapathy A.S. and Kumari, S. (2000) *Guidelines on Standard Operating Procedures for Clinical Chemistry*. Regional Office for South-East Asia, New Delhi: World Health Organization, p. 59-62.

Kozich J.J., Westcott S.L., Baxter N.T., Highlander S.K., and Schloss P.D. (2013) Development of a dual-index sequencing strategy and curation pipeline for analyzing amplicon sequence data on the miseq illumina sequencing platform. *Appl Environ Microb* **79(17)**, 5112-5120.

Krajewska, B. (2018) Urease-aided calcium carbonate mineralization for engineering applications: a review. *J Adv Res* **13**, 59-67.

Lauchnor, E., Schultz, L., Bugni, S., Mitchell, A., Cunningham, A., and Gerlach, R. (2013) Bacterially induced calcium carbonate precipitation and strontium coprecipitation in a porous media flow system. *Environ Sci Technol* **47**, 1557-1564.

Lueders, T., Manefield, M., and Friedrich, M.W. (2004) Enhanced sensitivity of DNA- and rRNA-based stable isotope probing by fractionation and quantitative analysis of isopycnic centrifugation gradients. *Environ Microbiol* **6(1)**, 73-78.

Lloyd A.B., and Sheaffe M.J. (1973) Urease activity in soils. *Plant Soils* **39**, 71–80.

Martin D., Dodds K., Ngwenya B., Butler I., and Elphick S. (2012) Inhibition of *Sporosarcina pasteurii* under anoxic conditions: implications for subsurface carbonate precipitation and remediation via ureolysis. *Environ Sci Technol* **46**, 8351–8355.

Martin D., Dodds K., Butler I.B., and Ngwenya B.T. (2013) Carbonate precipitation under pressure for bioengineering in the anaerobic subsurface via denitrification. *Environ Sci Technol* **47**, 8292-8699.

Mitchell A.C., Dideriksen K., Spangler L., Cunningham A., and Gerlach R. (2010) Microbially enhanced carbon capture and storage by mineral-trapping and solubility-trapping. *Environ Sci Technol* **44**, 5270–5276.

Mobley H.L., and Hausinger R.P. (1989) Microbial ureases: significance, regulation, and molecular characterization. *Microbiol Rev* **53**, 85–108.

Mortensen B., Haber M., DeJong J., Caslake L., and Nelson D. (2011) Effects of environmental factors on microbial induced calcium carbonate precipitation. *J Appl Microbiol* **111**, 338–349.

Phillips, A.J. (2013a) Biofilm-Induced Calcium Carbonate Precipitation: Application in the Subsurface. Ph.D. Dissertation, Montana State University, Bozeman, MT.

Phillips A.J., Lauchnor E., Eldring, J., Esposito M., Mitchell A.C., Gerlach R., Cunningham A.B., and Spangler L.H. (2013b) Potential CO2 leakage reduction through biofilm-induced calcium carbonate precipitation. *Environ Sci Technol* **47**, 142−149.

Phillips A.J., Cunningham A.B., Gerlach R., Hiebert R., Hwang C., Lomans B.P., Westrich J., Mantilla C., Kirksey J., Esposito R., and Spangler L.H. (2016) Fracture sealing with microbially-induced calcium carbonate precipitation: A Field Study. *Environ Sci Technol* **50**, 4111−4117.

Phillips, A. J., Troyer, E., Hiebert, R., Kirkland, C., Gerlach, R., Cunningham, A. B., Spangler, L., Kirksey, J., Rowe, W., and Esposito, R. (2018). Enhancing wellbore cement integrity with

551 microbially induced calcite precipitation (MICP): A field scale demonstration. *J Petroleum Sci*
552 *Eng* **171**, 1141-1148.
553
554 Rusu C., Cheng X., and Li M. (2011) Biological clogging in Tangshan sand columns under salt
555 water intrusion by *Sporosarcina pasteurii*. *Adv Mater Res* **250**, 2040–2046.
556
557 Stocks-Fischer S., Galinat J., and Bang S. (1999) Microbiological precipitation of $CaCO_3$. *Soil*
558 *Biol Biochem* **31**, 1563–1571.
559
560 Tobler D.J., Cuthbert M.O., Greswell R.B., Riley M.S., Renshaw J.C., Handley-Sidhu S., and
561 Phoenix V.R. (2011) Comparison of rates of ureolysis between *Sporosarcina pasteurii* and an
562 indigenous groundwater community under conditions required to precipitate large volumes of
563 calcite. *Geochim Cosmochim AC* **75**, 3290–3301.
564
565 van Paassen L.A., Daza C.M., Staal M., Sorokin D.Y., van der Zon W., and Loosdrecht M.C.M.
566 (2010) Potential soil reinforcement by biological denitrification. *Ecol Eng* **36**, 168–175.
567
568 Whiffin V.S., van Paassen L., and Harkes M. (2007) Microbial carbonate precipitation as a soil
569 improvement technique. *Geomicrobiol J* **24**, 417–423.

570 Wright D.T. and Wacey D. (2005) Precipitation of dolomite using sulphate-reducing bacteria from
571 the Coorong Region, South Australia: significance and implications. *Sedimentology* **52(5)**, 987-
572 1008.

573 Yoon, J.H, Lee, K.C., Weiss, N., Kho, Y.H., Kang, K.H., and Park, Y.H. (2001) *Sporosarcina*
574 *aquimarina* sp. nov., a bacterium isolated from seawater in Korea, and transfer of *Bacillus*
575 *globisporus* (Larkin and Stokes 1967), Bacillus psychrophilus (Nakamura 1984) and *Bacillus*
576 *pasteurii* (Chester 1898) to the genus *Sporosarcina* as Sporosarcina globispora comb. nov.,
577 *Sporosarcina psychrophila* comb. nov. and *Sporosarcina pasteurii* comb. nov., and emended
578 description of the genus *Sporosarcina*. *Int J Syst Evol Micr* **51**, 1079-1086.

579 Zeng Z. and Tice M.M. (2014) Promotion and nucleation of carbonate precipitation during
580 microbial iron reduction. *Geobiology* **12(4)**, 362-371.

581

582

583

584

585

586

587

Tables

Table 1. Summary of urea hydrolysis rates

Enrichment/Culture	Rate (moles urea hydrolyzed $cell^{-1}$ h^{-1})	Lag time
SL2 Facultative	$1.05 \cdot 10^{-10}$ +/- $1.70 \cdot 10^{-11}$	<2 hr
SL2 Anaerobic	$3.05 \cdot 10^{-10}$ +/- $2.40 \cdot 10^{-11}$	<2 hr
S. pasteurii	$1.94 \cdot 10^{-10}$ +/- $8.20 \cdot 10^{-12}$	2 hr

Figure Legends

Figure 1. Liquid analysis of SL2 enrichment cultures (CMM medium, pH 6, 50 g l^{-1} NaCl, 333 mmol l^{-1} Urea) with 0.033 mol l^{-1} $CaCl_2$*$2H_2O$. (**A**) Urea, (**B**) pH, (**C**) dissolved calcium levels, and **(D)** alkalinity were tracked every two hours in facultative (white symbols) and anaerobic (black symbols) enrichments from Soap Lake location SL2. An uninoculated abiotic control (diamonds) was also included to assess the potential for abiotic ureolysis and precipitation.

Figure 2. OD_{600nm} measured after 24 hours for facultative (**A, D**) and anaerobic (**B, E**) SL2 enrichments, as well as *S. pasteurii* strain ATCC 11859 (**C, F**). Shown are the maximal optical densities for salinity (▲), temperature (■), and pH (•) determined as specified in the materials and methods section.

Figure 3. Taxonomic diversity and richness at sampling site SL2 at the time of sample collection (baseline community) and following enrichment under facultative and anaerobic conditions. The left panel shows species-level diversity and richness in full-length 16S rRNA clone libraries from the enrichment cultures, while the right panel depicts genus-level 16S rRNA genes identified from Illumina-sequenced amplicon libraries. Only genera with a relative abundance ≥1% are shown.

Figure 4. Microbial communities enriched from an aqueous sample collected on the southeast shore of Soap Lake (site SL2). Field-Emission Scanning Electron Microscopy (FE-SEM) images of SL2 samples enriched under **(A)** facultative and (**B**) anaerobic conditions indicate the presence of numerous rod-shaped morphologies under both enrichment conditions.

Figure Legends for Supporting Information

Figure S1. Soap Lake location and the sites selected for sample enrichment. The map (**A**) illustrates Soap Lake and surrounding areas with an arrow depicting the approximate location of sites SL2, SL3, and SL4 while images and inset (**B**) highlight the precise sampling location of site SL2.

Figure S2. Raman spectra shown for mineral precipitates formed in facultative (**A**) and anaerobic (**B**) SL2 enrichments. A reference spectrum for calcite is displayed in orange while the acquired spectra are displayed in black.

Figure S3. Relative abundance of major genus-level clades at two high pH and high salinity locations in the Soap Lake (WA) drainage. The relative abundance of a genus is proportional to the area of the circle, as depicted by the scale bar on the bottom. Only genera with a relative abundance ≥1% are shown.

Table S1. Aqueous Geochemistry

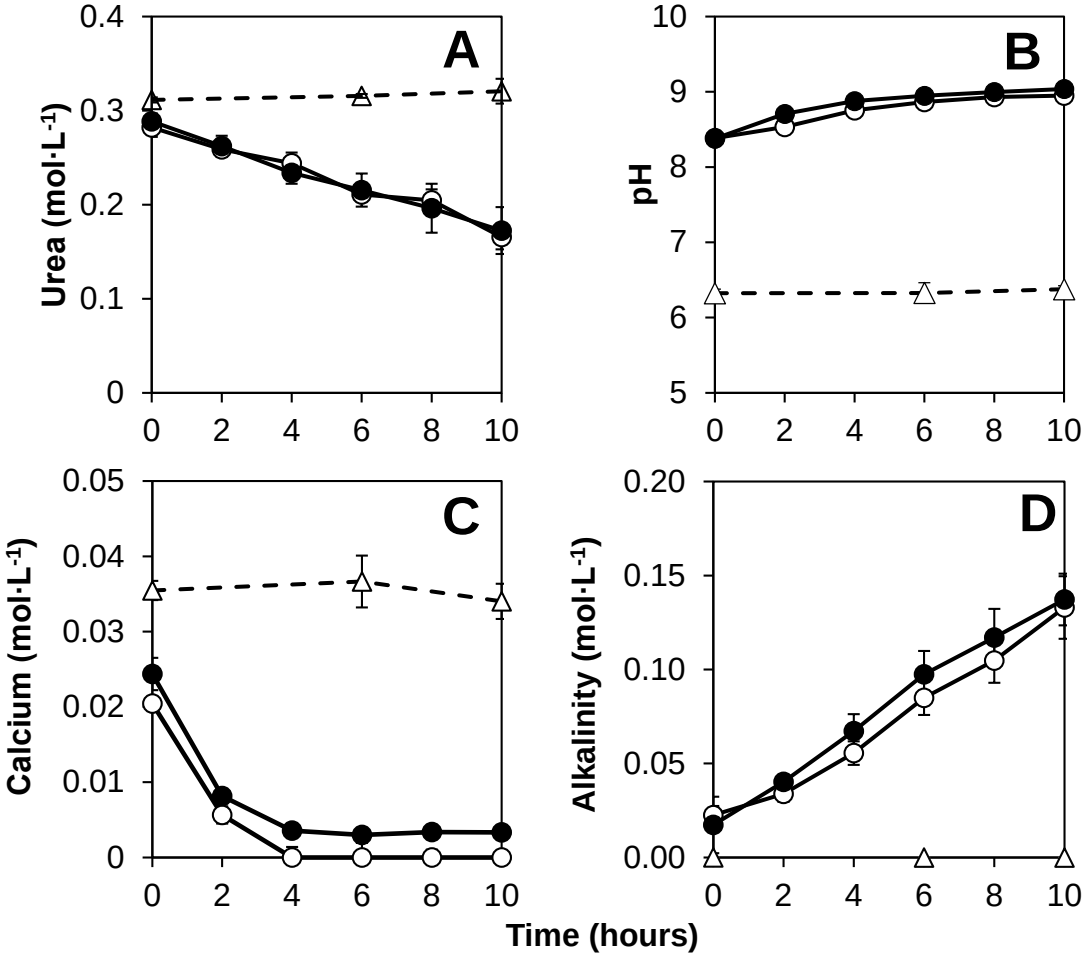

Figure 1. Liquid analysis of SL2 enrichment cultures (CMM medium, pH 6, 50 g·L^{-1} NaCl, 333 mmol·L^{-1} Urea) with 0.033 mol·L^{-1} $CaCl_2$*$2H_2O$. (**A**) Urea, (**B**) pH, (**C**) dissolved calcium levels, and (**D**) alkalinity were tracked every two hours in facultative (white symbols) and anaerobic (black symbols) enrichments from Soap Lake location SL2. An uninoculated abiotic control (diamonds) was also included to assess the potential for abiotic ureolysis and precipitation.

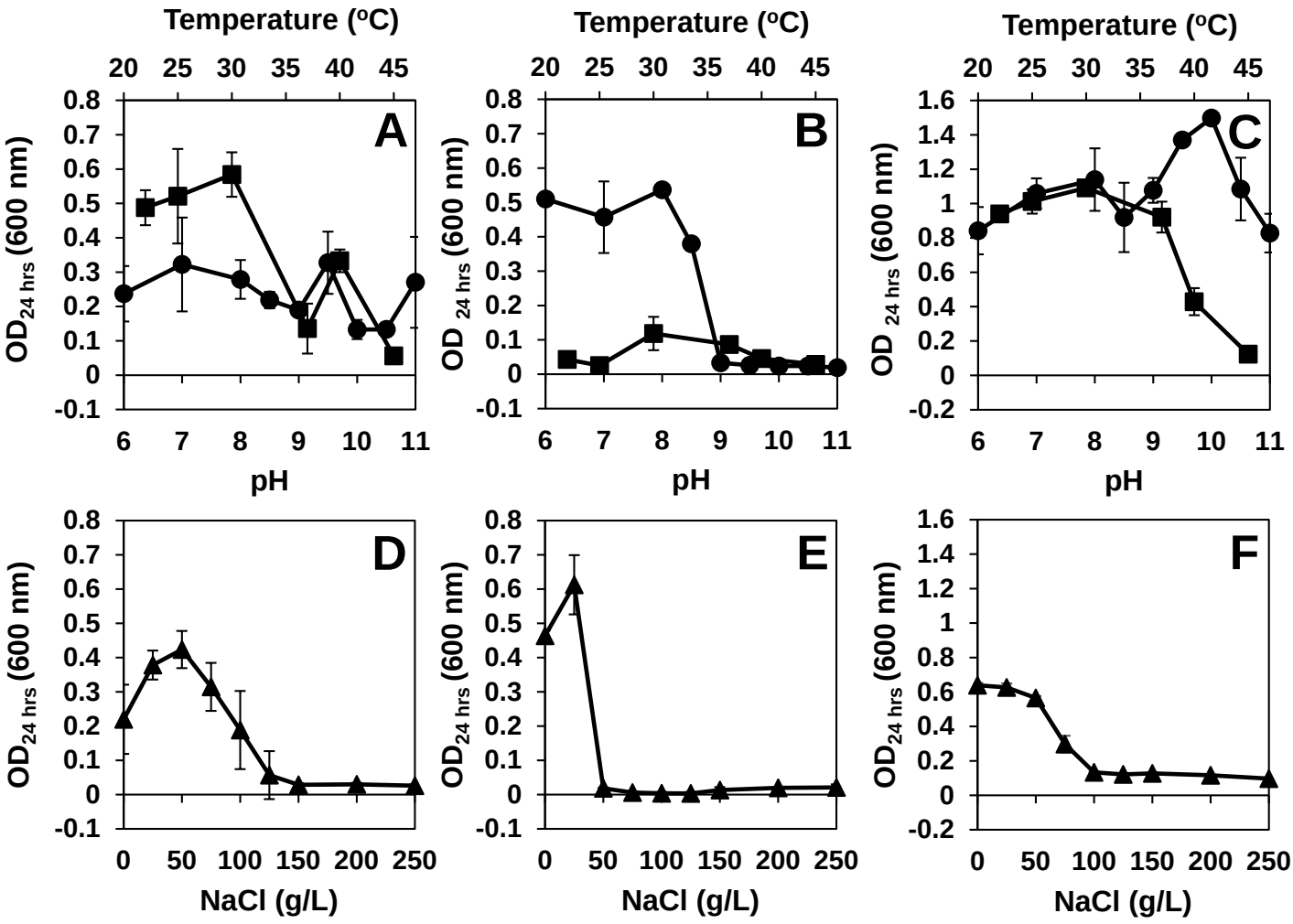

Figure 2. $OD_{600\ nm}$ measured after 24 hours for facultative (**A, D**) and anaerobic (**B, E**) SL2 enrichments, as well as *S. pasteurii* strain ATCC 11859 (**C, F**). Shown are the maximal optical densities for temperature (■), pH, (●) and salinity (▲) determined as specified in the materials and methods section.

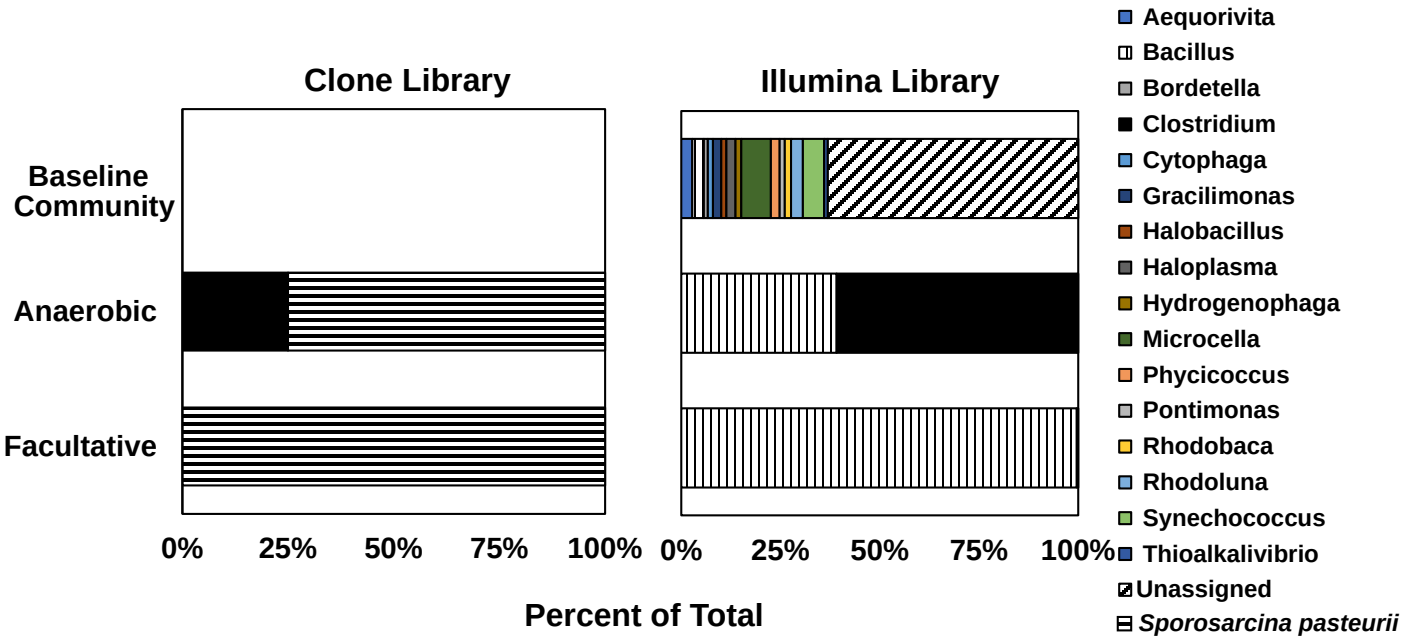

Figure 3. Taxonomic diversity and richness at sampling site SL2 at the time of sample collection (baseline community) and following enrichment under facultative and anaerobic conditions. The left panel shows species-level diversity and richness in full-length 16S rRNA clone libraries from the enrichment cultures, while the right panel depicts genus-level 16S rRNA genes identified from Illumina-sequenced amplicon libraries. Only genera with a relative abundance ≥1% are shown.

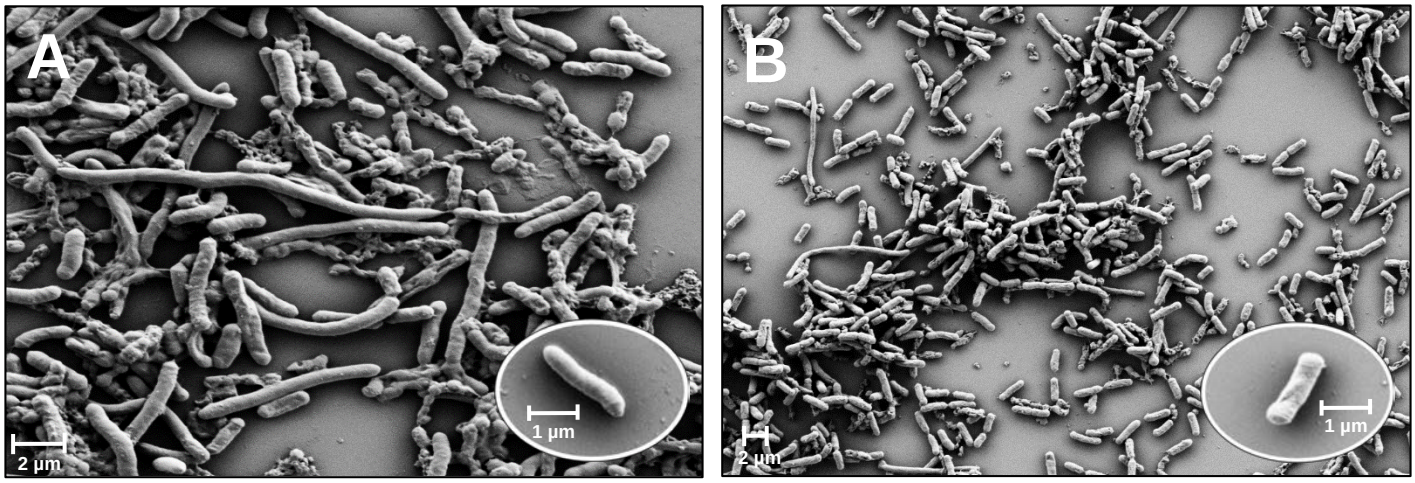

Figure 4. Microbial communities enriched from an aqueous sample collected on the southeast shore of Soap Lake (site SL2). Field Emission Scanning Electron Microscopy (FE-SEM) images of SL2 samples enriched under (**A)** facultative and (**B**) anaerobic conditions indicate the presence of numerous rod-shaped morphologies under both enrichment conditions.

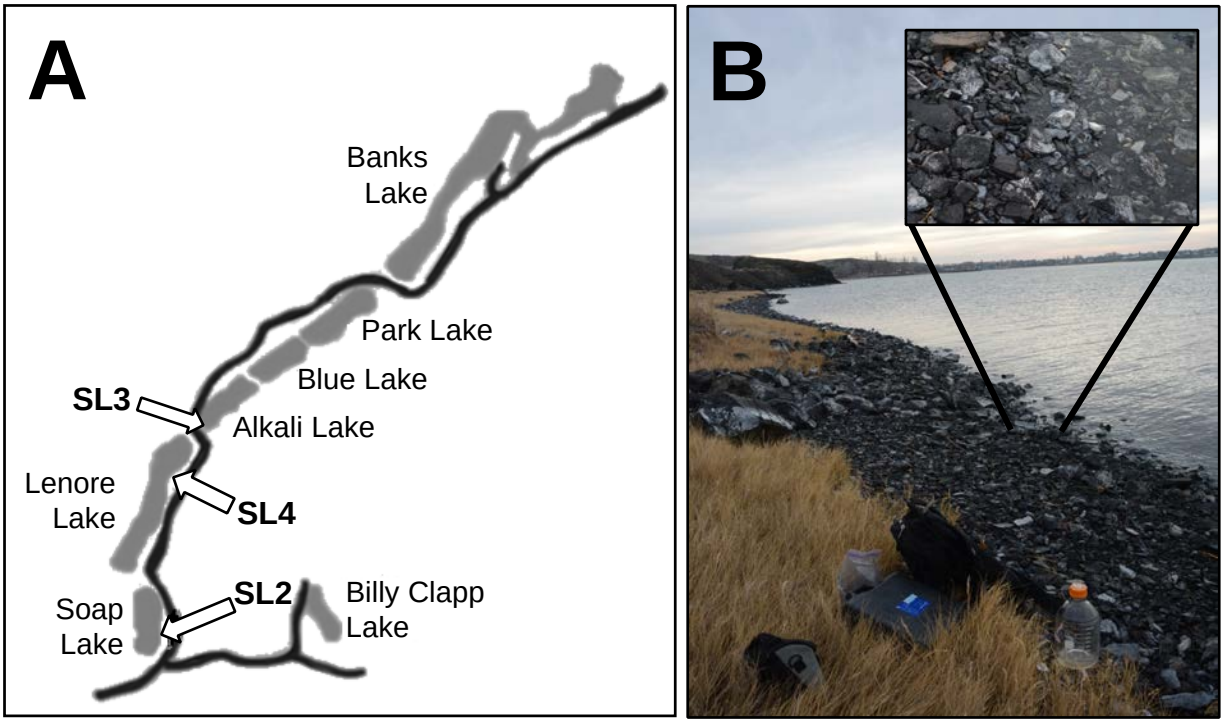

Figure S1. Soap Lake location and the sites selected for sample enrichment. The map (**A**) illustrates Soap Lake and surrounding areas with an arrow depicting the approximate location of sites SL2, SL3, and SL4 while images and inset (**B**) highlight the precise sampling location of site SL2.

.

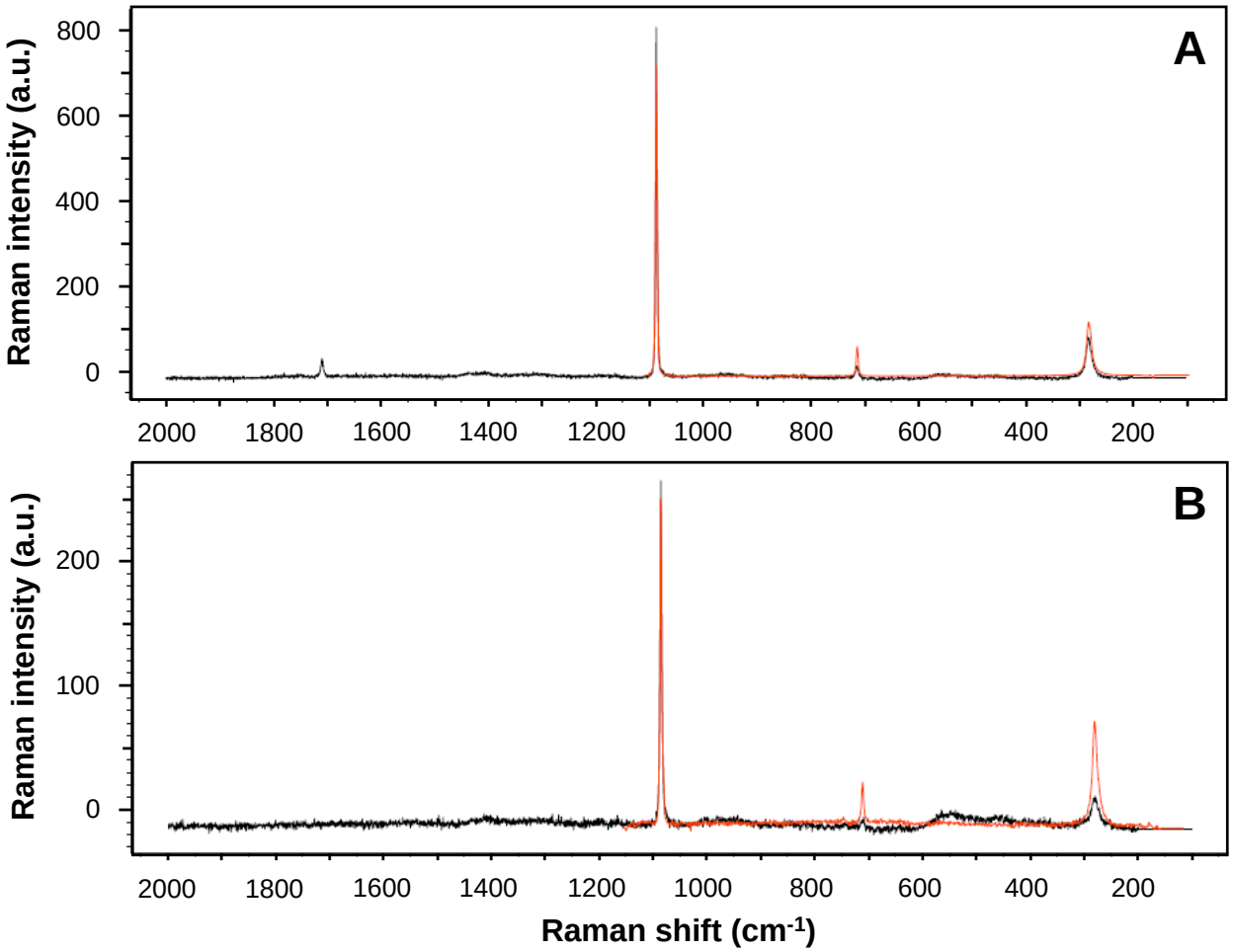

Figure S2. Raman spectra shown for mineral precipitates formed in facultative (**A**) and anaerobic (**B**) SL2 enrichments. A reference spectrum for calcite is displayed in orange while the acquired spectra are displayed in black.

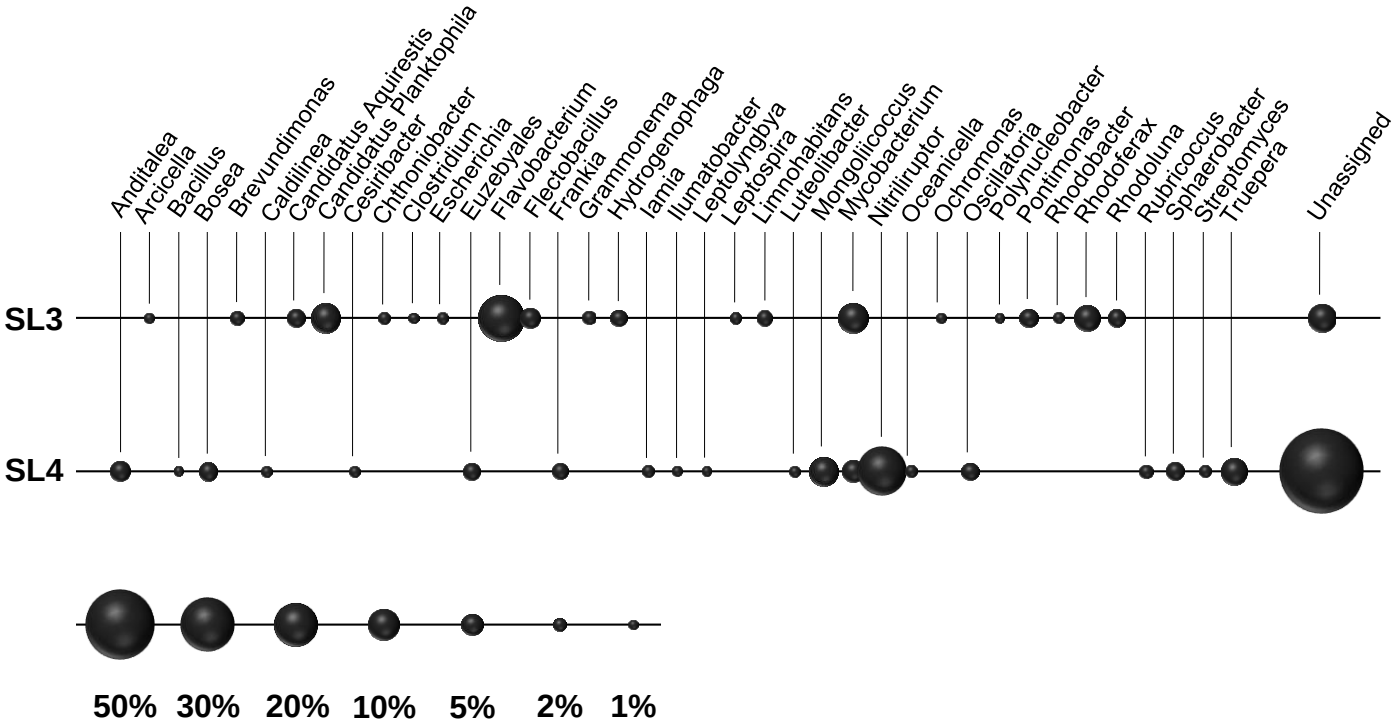

Figure S3. Relative abundance of major genus-level clades at two high pH and high salinity locations in the Soap Lake (WA) drainage. The relative abundance of a genus is proportional to the area of the circle, as depicted by the scale bar on the bottom. Only genera with a relative abundance ≥1% are shown.

Table S1. Aqueous Geochemistry

Constituent	**units**	**SL2**	**SL3**
pH		9.85	9.05
Temperature	^{o}C	2.0	1.8
Conductivity	mV	-115.2	-75.2
Cl^-	mmol l^{-1}	57.7	0.7
F^-	µmol l^{-1}	419.1	88.7
NO_3^-	µmol l^{-1}	116.2	35.6
SO_4^{2-}	mmol l^{-1}	537.9	4.1
Ca	µmol l^{-1}	62.4	405.2
Mg	mmol l^{-1}	0.12	1.71
Na	mmol l^{-1}	231.4	6.5
K	mmol l^{-1}	13.1	0.7
Se	µmol l^{-1}	64.1	0.8